Freeze-Thaw Performance of 3D Printed Concrete: Influence of Interfaces

Arnesh Das(✉), Asel Maria Aguilar Sanchez, Timothy Wangler, and Robert J. Flatt

Institute for Building Materials, ETH Zurich, Zurich, Switzerland
dasa@ethz.ch

Abstract. The long-term performance of 3D printed concrete structures is essential and among the various durability issues, frost damage is one of key importance, especially in cold locations such as Switzerland. For 3D printed materials, the presence of layer interfaces and cold joints is a potential issue in terms of frost resistance. Therefore, after extrusion, both cast and printed samples were prepared, and they were subjected to 300 cycles of freeze-thaw in accordance with ASTM C666. It was found that printed samples have lower resistance to freeze-thaw conditions compared to their cast counterparts. The lower resistance of the printed samples could be attributed to the heterogeneity in the microstructure, in particular to the higher capillary porosity in the interface region compared to that in the bulk. The higher capillary porosity could be confirmed based on the sorptivity test results.

Keywords: 3D printing · Frost damage · Interface · Capillary porosity

1 Introduction

3D concrete printing offers several advantages over conventional construction methods, and this is the reason why interest in this field has been flourishing in the recent years [1–4]. The recent years have seen enough success with regard to fabrication of structures by this method, however, the proper long-term performance of the structures from the point of view of both strength and durability is equally crucial. The literature mentions about some studies whereby the mechanical properties of 3D printed structures were investigated [5, 6], but studies concerning the durability aspect are still quite limited.

Among the various durability issues, frost damage is one of key importance, especially in cold locations such as Switzerland. For 3D printed materials, the presence of layer interfaces and cold joints is a potential issue in terms of frost durability. Deterioration of concrete saturated with water (or deicing salts) can take place through exposure to cyclic freezing temperatures. One of the major ways of mitigating frost damage is to use air-entraining admixtures (AEAs) whereby the entrained micro-sized air bubbles in the concrete matrix help by reducing the distance over which water is pushed, which limits the magnitude of the expansive stress on the cement paste [7, 8].

R. Buswell et al. (Eds.): DC 2022, RILEM Bookseries 37, pp. 200–205, 2022.
https://doi.org/10.1007/978-3-031-06116-5_30

Concerning 3D printing with concrete, there are a number of processing steps involved such as pumping, acceleration/mixing and extrusion. As a first step, the effect of the various processing conditions on the air void system was studied and their implications concerning freeze-thaw behavior was assessed [9, 10]. Hardened air void analysis was done on samples prepared after each processing step (including both cast and printed samples). It was found that extruded cast and extruded printed samples have very comparable void systems and spatial distribution of voids. However, the previously conducted analysis had a certain limitation in that capillary porosity, particularly in the interface region was not characterized. Therefore, the present work was motivated by the intention of determining whether this inhomogeneous air void analysis may be sufficient for predicting frost resistance of 3D printed samples. For that we report data on both cast and printed samples that are subjected to actual freeze-thaw conditions. Samples with AEA were also considered. Additionally, results about the water absorption behavior of the samples are further included.

2 Materials and Methods

Experiments were done on both cast and printed samples. The role of AEA was also considered, whereby these admixtures were included in the accelerator paste. The AEA dosage was fixed at 0.2% by weight of cement. Concerning the mix used for printing, the maximum aggregate size was 2 mm, its volume fraction was 0.45 and the water to cement ratio was 0.38. For further details about mixture design, procedure followed for the printing process and groups of mixes investigated, readers can refer to our preceding publication on this work [9].

The freeze-thaw tests were conducted on extruded cast and extruded printed samples. Two samples of each mix group were used for the freeze-thaw test. The test protocol followed was in accordance with ASTM C666 (procedure B) [11] with little modifications, with respect to the operating temperatures of the cycles. The samples were fully saturated before starting the cycles. Each cycle lasted for 4 h meaning that 6 cycles were done in a day. The freezing of the samples was done in air at −20 °C while thawing was done at 20 °C while being immersed in water. Mass loss measurements was the basis for assessing damage and this was done once a week, so approximately after every 42 cycles.

Damaged pieces were analyzed by SEM imaging, with polished sections produced via vacuum impregnation with an epoxy resin to preserve the crack structure. Analysis was done with an SEM FEI QUANTA 200 3D at high vacuum.

For the water absorption tests, samples (sizes were similar to those used for freeze-thaw test) were first dried in the oven at 60 °C until constant mass. Sorptivity tests were then conducted by placing these samples on a tray with a water height of approximately 2–3 mm. Only the extruded cast and extruded printed samples (groups 3–6) were used for this test. For the printed samples, tests were done in two ways – one in which the interface layers were placed parallel to the direction of water movement and one for which it was perpendicular to the direction of water ingress. The gain in mass was noted after 1, 5, 10, 30, 60 and 90 min. The sorptivity values were calculated based on the

slope of gain in mass (per area of cross-section) and the square root of time in minutes, hence they are reported in units of g/cm^2/min$^{1/2}$. Additionally, all dried samples were completely immersed in water until saturation and % increase in mass was recorded.

3 Results and Discussion

Based on the hardened air void analysis conducted previously, the spacing factor was computed for each mix group. They were found to be 232 μm, 273 μm, 208 μm, 220 μm, 161 μm and 171 μm respectively for groups 1–6 [9, 10]. None of the cast samples (groups 1, 2, 3 and 5) showed any signs of damage and the mass remained constant. However, the printed samples (both with and without AEA) showed signs of damage even though their spacing factor values were much similar to their corresponding cast samples. The non-AEA sample showed first signs of damage after 168 cycles while for the AEA one, it was after 264 cycles. Figure 1 shows the variation of mass versus number of freeze-thaw cycles, while Fig. 2 shows an example of one of the printed samples at 0 and 300 cycles of freeze-thaw. As can be seen, damage mostly occurred in the form of surface scaling. The damaged pieces fell off from the outer surface of the layers and in most cases, the thickness of the damaged piece was similar to the thickness of each layer of the print. Figure 3 shows SEM images of the damaged pieces, where cracks can be seen to originate in the cement paste, which is expected in frost damage. The cracks follow an orientation parallel to the exposure surface and go through aggregate, however, it is not possible to determine if the cracks originate in the interface region or the bulk of the printed layer.

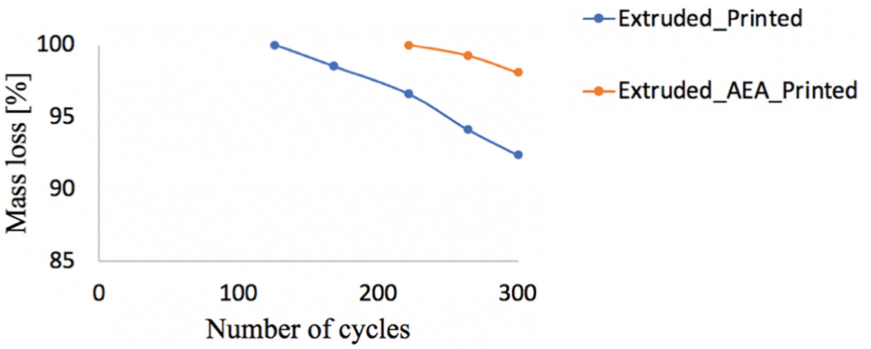

Fig. 1. Variation of mass with cycles of freeze-thaw for printed samples

The fact that only the printed samples showed signs of damage even though their spacing factors/void systems were similar to their cast counterparts indicates some degree of heterogeneity in the former. It is true that in most cases, spacing factor values directly translate to performance under freeze-thaw conditions, but the concept of spacing factor assumes that voids are mono-sized spheres uniformly distributed in the cement paste [12], hence it does not account for any heterogeneity. However, the resistance to frost damage is not solely influenced by distribution of entrained air voids but also on the volume of capillary porosity and the tensile strength.

Fig. 2. Samples at 0 cycles (left) and 300 cycles (right) of freeze-thaw. During thawing, samples were immersed in water in the same way as shown in picture with the surface having maximum area facing downward.

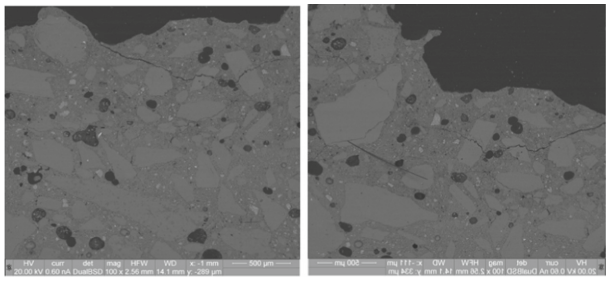

Fig. 3. SEM images of damaged printed sample after 300 cycles of freeze-thaw.

It is likely that the interface region in the printed samples has higher capillary porosity and is weaker compared to the bulk, which can explain its lower resistance to frost conditions. Table 1 shows the water absorption test results for the extruded cast and extruded printed groups of mixes. (It is to be noted that based on the analysis conducted previously, the cement paste content for all these mixes was found to be similar). When the samples are held in a perpendicular direction, the sorptivity values are quite similar to their cast counterparts. On the other hand, the printed samples show higher sorptivity when the interface lines are aligned in the direction of water ingress. The high volume of capillary pores is consistent the sorptivity test results. Further microstructure investigations would be required to determine the actual volume and distribution of capillary porosity, which was however beyond the scope of this work.

A similar observation about capillary porosity was made by Sanchez et al. [13], wherein they observed that the progression of carbonation front is much quicker in the interface region compared to that in the bulk. It could be argued that carbonation must have proceeded faster at the interface due to presence of entrapped voids. However, the rheology of the printed material used in their study was very similar to that in the present work and in either case, there were absolutely no signs of entrapped voids anywhere in the matrix. The rheology of the material after extrusion is fluid enough for large sized entrapped voids to easily escape.

Table 1. Water absorption test results for extruded cast and extruded printed groups of mixes. Second column shows condition of the sorptivity test for printed samples.

Sample name	Condition of testing	Sorptivity [g/cm^2/min$^{1/2}$]	% increase in mass [%] (complete immersion)
Acc_Extruded	–	0.008	6.6
Acc_Extruded_AEA		0.01	7.6
Acc_printed	Water ingress ⊥ layer interface	0.006	8.2
Acc_printed_AEA		0.014	8.2
Acc_Printed	Water ingress || layer interface	0.016	-
Acc_Printed_AEA		0.022	-

Concerning the water absorption test results, the general notion is that water movement in concrete takes place through the capillary pores and the entrained air voids do not take up any water [8, 14]. But entrained air voids may be filled with water for a material with open cell (interconnected air voids) network, which could be the case for low-density foamed concrete materials [15]. However, a contrasting observation is made for the cast samples wherein it is seen that mixes with higher AEA content have higher water absorption. This can be explained by the findings of Wong et al. [8] that air voids tend to affect packing of cement particles and thereby promote some degree of heterogeneity. The air void-paste interface region was found to locally have a much higher w/c ratio, similar to the interfacial transition zone (ITZ) found at the aggregate-paste interface. The higher proportion of entrained air voids may be thought of as inert inclusions (similar to increasing aggregate volume fraction) which do not influence transport properties of concrete but in fact, they can be connected through the much smaller sized capillary pores. The connectivity would essentially depend on the size of the voids entrained by the AEA. Additionally, it has also been reported in literature that air voids may also reach some degree of saturation if they have access to water for long enough period of time [8], which can explain the results of complete immersion in case of cast samples.

4 Conclusions

The hardened air void analysis revealed that extruded cast and extruded printed samples have similar void systems and spatial distribution of voids. The PPV analysis also predicted similar performance under freezing conditions. However, in order to validate the air void analysis results and also develop a better understanding of the effect of presence of interfaces in printed sample, conducting actual freeze-thaw tests was necessary. It was found that printed samples (both with and without AEA) have lower resistance to freeze-thaw conditions compared to their cast counterparts. The lower resistance of the printed samples could be attributed to the heterogeneity in the microstructure, in particular to the higher capillary porosity in the interface region compared to that in the bulk. The higher capillary porosity could be confirmed based on the sorptivity test results.

Acknowledgements. This research was supported by the NCCR Digital Fabrication, funded by the Swiss National Science Foundation. (NCCR Digital Fabrication, Agreement # 51NF40-141853). The authors would like to thank Concrete and Asphalt laboratory at EMPA, Switzerland for giving access to the freeze-thaw chamber and specially acknowledge the support provided by Janis Justs and Marcel Kappeli during the period of experiment at EMPA.

References

1. Khoshnevis, B.: Automated construction by contour crafting—related robotics and information technologies. Autom. Constr. **13**(1), 5–19 (2004). https://doi.org/10.1016/j.autcon.2003.08.012
2. Buswell, R.A., Leal de Silva, W.R., Jones, S.Z., Dirrenberger, J.: 3D printing using concrete extrusion: a roadmap for research. Cem. Concr. Res. 112, 37–49 (2018). https://doi.org/10.1016/j.cemconres.2018.05.006
3. Roussel, N.: Rheological requirements for printable concretes. Cem. Concr. Res. **112**, 76–85 (2018). https://doi.org/10.1016/j.cemconres.2018.04.005
4. Wangler, T., Lloret, E., Reiter, L., et al.: Digital concrete: opportunities and challenges. RILEM Tech. Lett. **1**, 67–75 (2016). https://doi.org/10.21809/rilemtechlett.2016.16
5. Feng, P., Meng, X., Chen, J., Ye, L.: Mechanical properties of structures 3D printed with cementitious powders (2015). https://doi.org/10.1016/J.CONBUILDMAT.2015.05.132
6. Van Der Putten, J., Deprez, M., Cnudde, V., De Schutter, G., Van Tittelboom, K.: Microstructural characterization of 3D printed cementitious materials. Materials **12**(18), 2993 (2019). https://doi.org/10.3390/ma12182993
7. Du, L., Folliard, K.J.: Mechanisms of air entrainment in concrete. Cem. Concr. Res. **35**(8), 1463–1471 (2005). https://doi.org/10.1016/j.cemconres.2004.07.026
8. Wong, H.S., Pappas, A.M., Zimmerman, R.W., Buenfeld, N.R.: Effect of entrained air voids on the microstructure and mass transport properties of concrete. Cem. Concr. Res. **41**(10), 1067–1077 (2011). https://doi.org/10.1016/j.cemconres.2011.06.013
9. Das, A., Song, Y., Mantellato, S., Wangler, T., Lange, D.A., Flatt, R.J.: Effect of processing on the air void system of 3D printed concrete. Cem. Concr. Res. **156**, 106789 (2022). https://doi.org/10.1016/j.cemconres.2022.106789
10. Das, A.: 3D concrete printing: early-age strength build-up and long-term durability, PhD thesis, (submitted). Published online (2022)
11. C09 Committee. Test method for resistance of concrete to rapid freezing and thawing. ASTM Int. https://doi.org/10.1520/C0666_C0666M-15
12. Powers, T.C., Helmuth, R.A.: Theory of volume changes in hardened portland-cement paste during freezing. Highw. Res. Board Proc. **32** (1953). https://trid.trb.org/view/102368. Accessed 30 Apr 2021
13. Microstructural examination of carbonated 3D-printed concrete – Sanchez. J. Microsc. Wiley Onl. Lib. https://doi.org/10.1111/jmi.13087. Accessed 4 Apr 2022
14. Nambiar, E.K., Ramamurthy, K.: Sorption characteristics of foam concrete. Cem. Concr. Res. **37**(9), 1341–1347 (2007)
15. Das, A.: Microstructure characterization of foamed cement and concrete (MS Thesis). Published online (2018)